Neodymium and Strontium Isotope Investigation of the Precambrian Kalkkloof Paleosol, South Africa

by

Katherine M. Walden

Submitted to the Graduate Faculty of

Arts and Sciences in partial fulfillment

of the requirements for the degree of

Master of Science

University of Pittsburgh

2005

UNIVERSITY OF PITTSBURGH

FACULTY OF ARTS AND SCIENCES

This thesis was presented

by

Katherine M. Walden

It was defended on

4-18-2005

and approved by

Brian W. Stewart

Thomas H. Anderson

Charles E. Jones

Rosemary C. Capo

Neodymium and Strontium Isotope Investigation of the Precambrian Kalkkloof Paleosol, South Africa

Katherine Walden, MS

University of Pittsburgh, 2005

The Precambrian Kalkkloof paleosol, South Africa, developed on an Archean ultramafic complex sometime before ~2.3 billion years (Ga) ago. This weathering profile is of great interest because it formed during a time when many workers believe atmospheric oxygen levels were rising to near-present day concentrations, and cerium (Ce) anomalies have been measured in Kalkkloof paleosol samples (Watanabe et al., 2003), indicating formation under high-O_2 conditions. In this study, I applied the samarium-neodymium (Sm-Nd) and rubidium-strontium (Rb-Sr) isotope systems to samples of the Kalkkloof paleosol and parent material. The goals of this study are to constrain the age of pedogenesis of the Kalkkloof paleosol, and to determine the extent to which rare earth elements (REE, including Ce) and other elements were mobilized during and after pedogenesis. Titanium-normalized concentration patterns for Sm and Nd are consistent with accumulation of REE in the lower portions of the weathering profile during its formation. Isotopic analysis of eight whole-rock Kalkkloof samples, including the parent ultramafic material, indicates that the Sm-Nd and Rb-Sr systematics have been disturbed by at least two geological events subsequent to formation of the ultramafic parent, and no meaningful ages were obtained. These events are likely to include weathering and formation of the paleosol around 2.5 Ga ago, and later metamorphism associated with intrusion of the Bushveld igneous complex around 2 Ga ago. The four samples with the highest concentrations of Nd (>1 ppm) have $\in_{Nd}$(2.5 Ga) values that are consistent with REE fractionation during weathering around 2.5

Ga ago. These four samples also contain significant Ce anomalies. Preservation of REE systematics could result if the REE were concentrated in relatively resistant trace phases such as phosphates. Thus, the data are consistent with a high-O_2 atmosphere (leading to Ce oxidation) when the paleosol formed >2.3 Ga ago. To a first approximation the Rb-Sr data are consistent with the multi-stage history suggested by the Sm-Nd data. The Rb-Sr results further suggest that the Kalkkloof rocks were at least mildly affected by metamorphism and/or weathering events that ended no earlier than about 1.7 Ga ago.

TABLE OF CONTENTS

LIST OF TABLES

LIST OF FIGURES

1. KALKKLOOF PALEOSOL: INTRODUCTION AND BACKGROUND

1.1. Introduction

Paleosols, weathering or soil profiles that have been preserved in the geologic record, are products of interactions among the Earth's atmosphere, hydrosphere, lithosphere and biosphere. The mineralogy and chemistry of paleosols can provide information about atmospheric composition and terrestrial environmental conditions at the time they formed (Holland, 1984; Ohmoto, 1996; Rye and Holland, 1998). During weathering, rocks are physically disrupted and chemically altered or dissolved. Certain elements tend to exhibit mobile behavior during weathering (*e.g.*, alkali and alkaline earth elements) whereas others tend to remain in place (*e.g.*, high charge/radius ions such as Al^{3+}, Ti^{4+}, and the REE^{3+}). Mobile ions can be leached from the upper horizons of a weathering profile and redeposited into lower horizons during chemical weathering. In detail, ion mobility depends on many factors including temperature, Eh, pH, and atmospheric composition, and any element can be mobilized during soil formation given the right conditions. Elements such as iron, vanadium, and cerium behave differently in oxidized and reduced states, and therefore may provide information about oxygen levels in the atmosphere at the time of formation of the paleosol. For example, Fe^{2+} in the presence of O_2 becomes oxidized to a 3+ state and is then relatively immobile. In a reducing environment, iron remains in the 2+ state and is expected to be leached from the upper portions of a soil profile (Holland, 1984; Gutzmer and Beukes, 1998; Yang et al., 2002).

Precambrian paleosols can be difficult to identify as paleosols because most rocks of this age have undergone one or more episodes of metamorphism and deformation. These processes

can alter or destroy original pedogenic textures and chemical profiles. Rye and Holland (1998) have developed criteria for positively identifying a Precambrian paleosol worthy of paleo-atmosphere study: (1) it must have developed on a homogenous bedrock and be preserved in place; (2) it must exhibit changes in mineralogy, chemical composition, and texture that are consistent with soil forming processes; and (3) there must be identifiable evidence that this unit was exposed at the surface.

Paleosols from 2.0 to 2.4 Ga ago have been intensely studied to document a possible major rise in atmospheric oxygen levels (*e.g.*, Holland, 1984; Lambert and Donelly, 1991; Kahru and Holland, 1996; Rye and Holland, 1998; Farquhar et al., 2000; Murakami et al., 2001; Towe, 2002; Wiechert, 2003; Bekker et al., 2004). For example, the Pronto paleosol (2.6 – 2.45 Ga), developed on Archean granites in Canada, contains Ce in a reduced (3+) state in the mineral rhabdophane. This is used as evidence that this paleosol formed under reducing conditions (Murakami et al 2001). Laterites in the paleokarst depressions on the Cambellrand Dolomite (2.0 – 2.2 Ga), Transvaal Supergroup South Africa, contain ferric oxides that are interpreted as evidence for an oxygenated environment (Gutzmer and Beukes 1998). The age differences between these deposits leaves a considerable gap in time during which oxygen levels may have risen.

This study focuses on the radiogenic isotope systematics of the Precambrian Kalkkloof paleosol of South Africa. The Kalkkloof paleosol formed on ultramafic bedrock of the Onverwacht Supergroup (>2.7 Ga) and is overlain by sedimentary rocks of the Transvaal Supergroup (2.3 Ga) (Martini 1994). Studies of the Kalkkloof paleosol have revealed cerium anomalies (Watanabe et al., 2003) that suggest an oxidative surface environment at the time of rare earth element (REE) fractionation. In this study, I use the Sm-Nd and Rb-Sr isotopic

systems to the Kalkkloof paleosol in order to (1) place constraints on the timing of REE fractionation and cerium oxidation (*i.e.*, pedogenesis); (2) determine possible effects of post-pedogenic metamorphism on paleosol geochemistry; and (3) evaluate the degree to which the present-day chemistry of the profile reflects Precambrian pedogenic processes and conditions.

1.2. Background

1.2.1. Area Geology

The Kalkkloof paleosol is located in South Africa on the Kaapvaal craton about 50 km west of Barberton (Fig. 1-1). The layered ultramafic complex on which it formed is part of the Onverwacht Supergroup (Menell et al., 1986). This supergroup includes the Barberton Greenstone Belt, which is about 50 km east of the paleosol (Fig. 1-2). The Kalkkloof layered ultramafic complex was originally part of the Barberton Greenstone Belt, but it was separated from the main mass by intrusive granites of the Nelshoogte Pluton, part of the Archean granite-gneiss complex that intruded about 3.2 Ga ago (Menell et al., 1986). The ultramafic complex was apparently intruded into volcanics of the Onverwacht Supergroup (Martini, 1994).

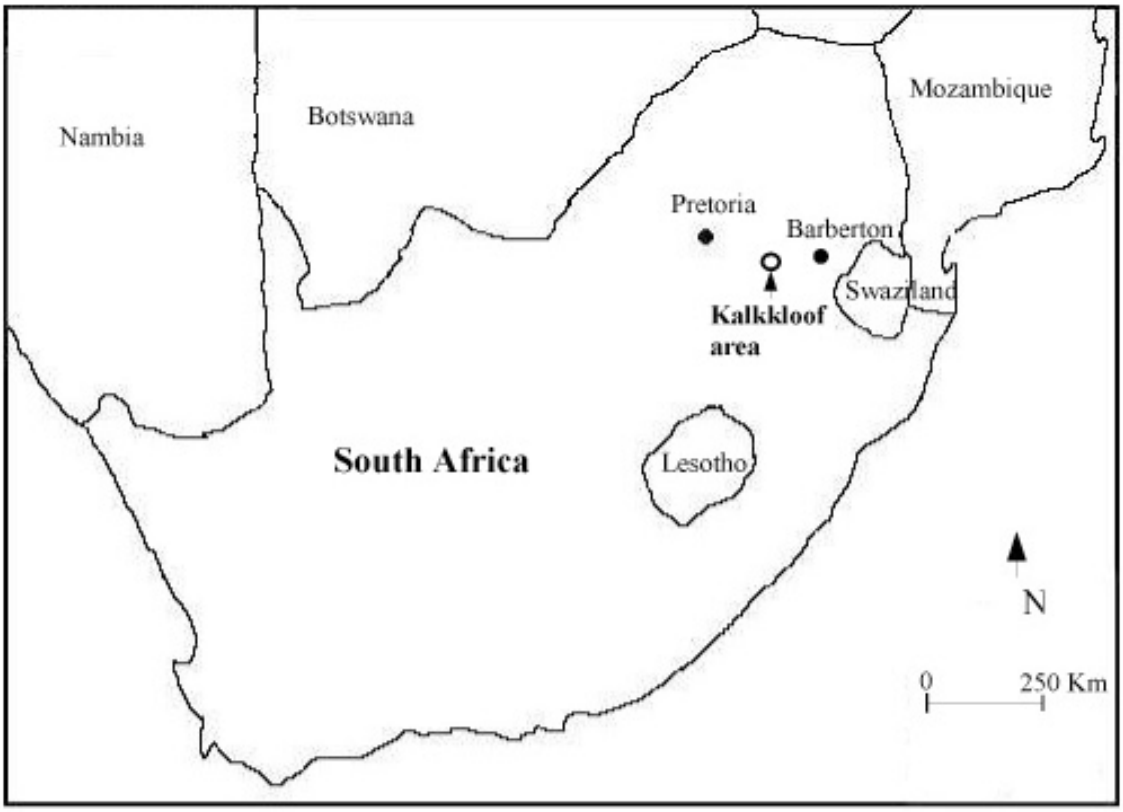

Figure 1-1: Location map of the Kalkkloof paleosol.

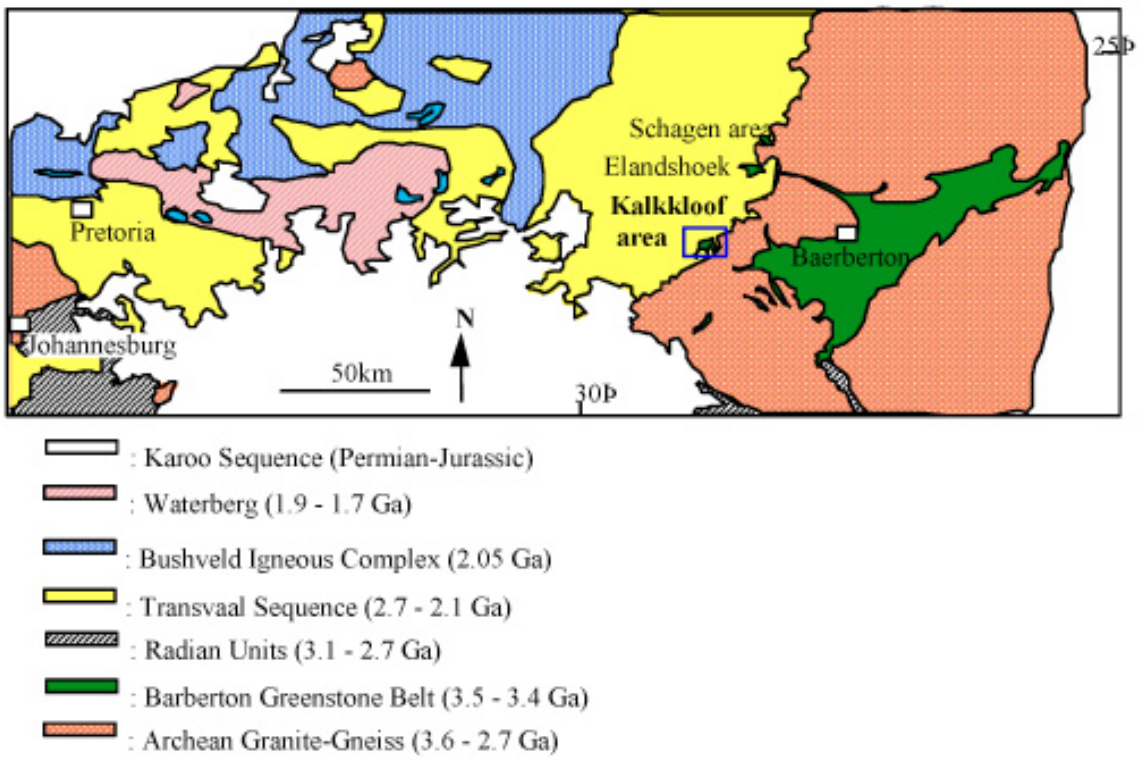

Figure 1-2: Geologic map showing the Barberton Greenstone Belt, Transvaal Sequence, Archean granite-gneiss, and the Kalkkloof area (modified after Martini, 1994 and Watanabe et al. ,2000).

The Barberton Greenstone Belt is made up of cherts, highly altered and sheared volcanic rocks, pyroclastics, and intrusive igneous rocks (Lowe and Byerly, 1999). This belt formed during volcanism in response to accretion of "protocontinental" blocks and underplating (Lowe, 1999b). In the belt area, ultramafic rocks generally form valleys and granitoid rocks form ridges (Button and Tyler, 1981). The ultramafic magmas have undergone olivine, orthopyroxene, and in some cases clinopyroxene fractionation (Lowe, 1999b). Some serpentinized rocks show evidence for sub-sea-floor metasomatism (Byerly, 1999). Others show evidence, such as current structures, for formation in shallow waters (Byerly, 1999).

The Transvaal Supergroup overlies the Kalkkloof paleosol (Fig. 1-3). It consists of sedimentary rocks that were accumulated under marine to subaerial conditions (Reimer, 1988) in an elongate east-west basin (Haughton, 1969). Granitoids emplaced 3.0 Ga ago and 2.8 - 2.6 Ga ago were the most important contributors to the Kaapvaal Craton sediments, including the Transvaal supergroup (Condie and Wronkiewicz, 1990). Deposition of the Transvaal Supergroup began 2.5 – 2.6 Ga ago (Jahn et al., 1990; Klein and Buekes, 1990).

The Transvaal supergroup is broken up into the Chuniespoort group and the overlying Pretoria group (Martini, 1994). The Chuniespoort Group includes the Malmami subgroup which is primarily carbonates (Reimer, 1988 and Jahn et al., 1990) and the Black Reef formation (Martini, 1994). The Chuniespoort Group was deposited directly on top of the paleosol. Although it does not exist on top of the paleohill from which the Kalkkloof samples were taken (Martini, 1994), it does overlie the paleosol at the base of the paleohill (Fig. 1-3). Rip-up clasts of the paleosol rolled down the hill and were incorporated into the Chuniespoort Group (Martini 1994). The Chuniespoort Group is made up of marine platform sediments that are primarily carbonates (Buick et al., 1998).

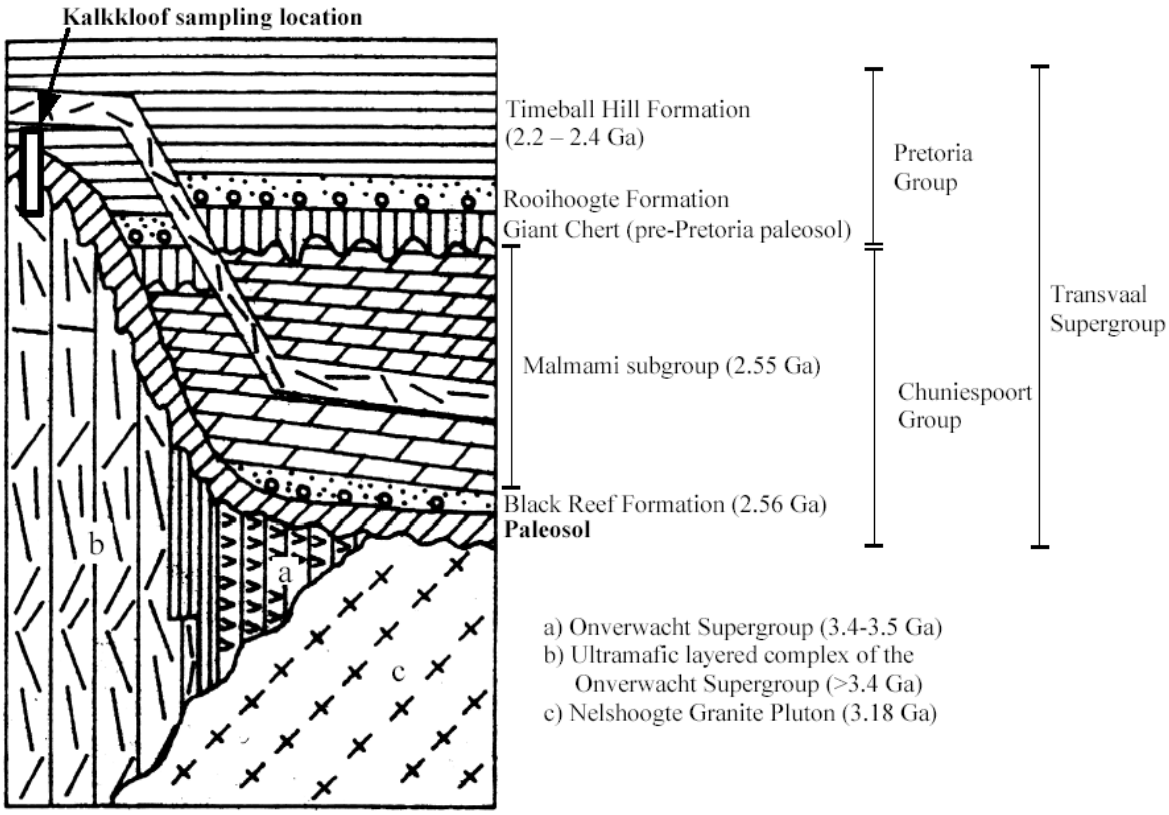

Figure 1-3: Idealized cross-section of the Kalkkloof paleosol area showing the unconformity between the Archean units and the Transvaal Sequence (modified after Martini, 1994).

The Pretoria Group is composed of the Giant Chert (pre-Pretoria paleosol), the Rooihoogte formation, and the overlying Timeball Hill formation. The shales of the Pretoria Group are mostly from marine to marginal marine environments (Button and Tyler, 1981) that were deposited following basin subsidence (Haughton, 1969). Shales from the Timeball Hill Formation of the Pretoria Group overlie the paleosol at the sampling location (Fig. 1-3; Martini, 1994; Watanabe, 2000).

1.2.2. Kalkkloof Paleosol

Paleosols developed in the Kalkkloof area vary from a few meters to about 50 meters thick (Martini, 1994). The paleosol is about fourteen meters thick at the location where samples were collected, and it formed on a paleohill about 150 m above the lower Onverwacht unit and the Nelshoogte Pluton (Fig. 1-3; Martini, 1994). Serpentinite hills in the area had a relief up to 100-150 m at the time the Transvaal sediments were deposited (Menell et al., 1986; Martini, 1994).

The paleosol in the Kalkkloof area is composed primarily of serpentinite. Some phosphate-bearing minerals, possibly monazite and rhabdophane, have been identified by SEM (Watanabe et al., 2003). The paleosol contains organic carbon, probably as fine graphite in the talc zones (Martini, 1994). A microbial mat may have helped to stabilize the soil and allow it to get as thick as it did (Martini, 1994).

The Kalkkloof paleosol does fit Rye and Holland's criteria (1998) for Precambrian paleosol. It developed on relatively homogeneous bedrock - the layered ultramafic complex of the Onverwacht Supergroup. The lower units of the paleosol retain dunite textures that change gradually towards the top of the paleosol (Martini, 1994). Evidence that this paleosol was exposed at the surface includes rip-up clasts from the paleosol that are contained in the overlying

sedimentary formation (Martini, 1994). Ratios of Al/Ti remain relatively show deviations of less than ±40% from the parent material throughout the profile (Watanabe, personal communication, 2004), which suggests weathering of uniform parent material.

The Kalkkloof paleosol developed on a protolith consisting of a layered ultramafic complex of the Onverwacht Supergroup. The Kalkkloof ultramafic layered complex consists of alternating serpentinized dunite and orthopyroxene layers with interlayers of talcose schists (Menell et al., 1986). Serpentinized dunite lies directly beneath the paleosol (Martini, 1994). Serpentinization took place before the paleosol formed. The age of the unconformity during which the paleosol formed is unknown. The paleosol has silcrete layers and a duricrust that suggest the soil formed in a semi-arid environment with alternating wet and dry periods (Martini, 1994). It is overlain by sediments of the Transvaal Supergroup (Fig. 1-2).

1.2.3. Kalkkloof Paleosol age constraints

For a summary of depositional ages and metamorphic event ages, see Table 1-1. The protolith from which the paleosol formed is dunite that formed part of the ultramafic layered complex of the Onverwacht Supergroup. A Sm-Nd age of 3.56 ± 0.24 Ga has been reported for the beginning of volcanism in this formation (Jahn et al., 1982). Later volcanic rocks in the group have been dated with the Sm-Nd system to an age of 3.540 ± 0.030 Ga (Hamilton, 1979). The Timeball Hill Formation of the Pretoria Group that lies directly on top of the paleosol has an age of 2.2 to 2.4 Ga (Gutzmer and Buekes, 1998). The Black Roof Conglomerate, which has an age of 2.56 Ga, overlies the paleosol in areas away from the Kalkkloof section (Rye and Holland, 1998).

Table 1-1: Major events affecting the Kalkkloof paleosol and protolith.

Age (Ga)	Geologic Event
2.060 – 2.050	Intrusion of Bushveld Igneous Complex (Walraven et al. 1990; Button and Tyler 1981)
2.200	Continuing Transvaal deposition, complex step faulting and movement of serpentinites (Menell et al. 1986)
2.22 – 2.24	Rb-Sr age and Pb-Pb ages for lavas in the Pretoria Group (Jahn et al., 1990)
2.2 – 2.4	Timeball Hill Formation (Gutzmer and Buekes 1998)
2.370	Pb-Pb age of metamorphic and or hydrothermal event (Walraven et al. 1990)
2.55	Malmami Subgroup deposited (Martini 1994)
2.5 – 2.6	Pb-Pb age for beginning of Transvaal dolomite deposition (Jahn et al. 1990)
2.800	Metamorphic event from granitoid emplacement recorded in Vredefort basement rock and Dominion Group (Walraven et al 1990)
3.170 – 3.060	Thermal metamorphism and crustal addition through granitiod emplacement (Walraven et al. 1990)
3.180 ± 75	Rb-Sr age for Nelshoogte Pluton (granite intrusion between layered ultramafic complex and Barberton Greenstone Belt) with initial Sr ratio of 0.7010 (Menell et al. 1986)
3.220 ± 80	U-Pb zircon age of Nelshoogte Pluton (Menell et al 1986)
3.540 ± 30	Sm-Nd age of volcanics in the Onverwacht Supergroup (Hamilton, 1979)

The paleosol at the Kalkkloof location must have formed between 3.4 Ga and 2.2 to 2.4 Ga ago. A number of metamorphic events could have impacted the paleosol depending on when it formed. Main events include the intrusion of Nelshoogte Pluton 3.2 Ga ago (Menell et al., 1986) and faulting and movements of the serpentinites 2.20 Ga ago (Menell et al. 1986) and intrusion of the Bushveld Igneous Complex 2.060 to 2.050 Ga ago (Walraven et al. 1990; Button and Tyler 1981).

1.2.4. Geochemistry of rare earth elements in paleosols

The rare earth elements (REE) comprise a group of lithophile elements that exhibit similar chemical behavior, due to a stable 3+ valence and ionic radii that systematically decrease with atomic number (Henderson, 1984). They can be (but are not always) relatively immobile under weathering and metamorphic conditions (Humphris, 1984). To better describe fractionations resulting from geologic processes, REE are commonly divided up into the heavy rare earth elements (HREE), which includes Gd through Lu, and the light rare earth elements (LREE), which includes La through Sm (Henderson, 1984).

The REE concentrations reflect the mineralogy and petrogenesis of the rocks. It is assumed that the bulk Earth started out with chondritic REE concentrations when it formed. REE were fractionated when the Earth differentiated and most terrestrial rocks today do not have chondritic REE concentrations. The continental crust is enriched in all REE and especially in the LREE (Henderson, 1984). The mantle is correspondingly depleted in REE and especially in LREE relative to crustal rocks. This mantle depletion is commonly reflected in ultramafic rocks. REE concentrations in ultramafic rocks can range from less than 0.001 to 10 times the chondritic

value (Frey 1984). The USGS standard dunite has REE abundances ranging from 0.01 to 0.1 times the chondritic value. This dunite shows depletion in the middle REE (Pm through Ho), which appears to be standard for dunites and harzburgites reported in the literature (*e.g.*, Frey, 1984; Sharma et al., 1995; Melcher et al., 2002). In general, serpentinization does not appear to have a significant effect on REE concentrations (Suen and Frey 1987). Harzburgites in the Eastern Alps are typically enriched in LREE regardless of their degree of serpentinization (Melcher et al., 2002). In some cases, however, heavy serpentinization associated with seafloor hydrothermal alteration appears to have led to REE loss (Ottonello et al., 1979).

Most REE in ultramafic rocks are found in clinopyroxenes (Cullers and Graf, 1984). In some cases, REE and especially LREE are concentrated in phosphate minerals such as apatite ($Ca_5(PO_4)_3(F,Cl,OH)$) and monazite ($(Ca,La,T,Th)PO_4$) (Braun et al., 1993; Jonasson et al., 1985). HREE can be concentrated in the mineral xenotime (YPO_4) (Jonasson et al., 1985). Clays such as kaolinite and illite may preferentially adsorb LREE in weathering reactions (Nesbitt, 1979). Titanite shows enrichment in the middle REE (Braun et al., 1993).

Weathering processes can fractionate the HREE and LREE (Walter et al., 1995). Rare earth elements tend to be leached from upper horizons in a soil and concentrated in clay horizons during weathering (Condie et al., 1995; Braun et al., 1993). Feldspars, biotite, and apatite concentrate LREE in weathering rinds (Aubert et al. 2001). In general, light rare earth elements are more mobile than HREE at pH values between 6.5 and 8 (MacFarlane et al., 1994). The movement of REE, Th, and U during weathering processes is controlled by the stability of the accessory minerals that contain the bulk of the inventory in typical rocks (Pan and Stauffer, 2000; Panihi et al., 2000). If these minerals remain stable and unaffected by later metamorphism, they will preserve values from the time of their formation (Murakami et al., 2001).

Only the rare earth elements Eu and Ce commonly form non-trivalent cations. Under certain conditions, these elements exist as Eu^{2+} and Ce^{4+}. Cerium is especially significant for studies of paleosols because it deviates from trivalent behavior depending on the pH, Po_2, and temperature of the weathering solutions. Notably, Ce^{3+} can oxidize to Ce^{4+} under conditions found at the Earth's surface (Clark, 1984). During weathering, Ce^{4+} is insoluble and precipitates as the mineral cerianite ($CeO_{2)}$ (Braun et al., 1990), while the other REE may remain in solution. This can lead to a Ce anomaly, in which the normalized Ce concentration is elevated or depleted in concentration relative to its neighbor (La and Pr) in a normalized REE concentration plot. Negative Ce anomalies tend to form at weathering fronts and positive Ce anomalies tend to form at the tops of weathering profiles (Braun et al., 1990, 1998). If a Ce anomaly is observed, the inference is that REE fractionation took place at or near the Earth's surface under an oxygenated atmosphere. However, locally anoxic weathering conditions can and frequently do inhibit the formation of Ce anomalies even during weathering under today's high-O_2 atmosphere (Braun et al., 1990). Therefore, the presence of a Ce anomaly implies high atmospheric O_2 during weathering, but the absence of one does not require extremely low atmospheric O_2 levels.

1.2.5. Sm-Nd system

Samarium and neodymium are both rare earth elements. The nuclide ^{147}Sm decays to ^{143}Nd by the α process with a half-life of about 106 billion years. The ^{143}Nd abundance is generally normalized to the stable isotope ^{144}Nd. $\in_{Nd}(T)$ is a convenient way to express the $^{143}Nd/^{144}Nd$ ratio of a sample relative to the $^{143}Nd/^{144}Nd$ ratio of chondritic meteorites (assumed to be ≈ bulk Earth ≈ solar system) at any age T:

$$\varepsilon_{Nd}(T) = 10^4 \left[\frac{(^{143}Nd/^{144}Nd)_{sample}}{(^{143}Nd/^{144}Nd)_{CHUR}} - 1 \right] \quad (1.1)$$

where CHUR is the chondritic meteorite value (CHondritic Uniform Reservoir).

The present-day value for $(^{143}Nd/^{144}Nd)_{CHUR}$ measured at the University of Pittsburgh isotope geochemistry lab is 0.511847. Values can be corrected to the past using $^{147}Sm/^{144}Nd)_{CHUR}$ = 0.1967 and $\lambda_{Sm} = 0.00654$.

$$^{143}Nd/^{144}Nd_m = {}^{143}Nd/^{144}Nd_i + {}^{147}Sm/^{144}Nd(e^{\lambda t}-1) \quad (1.2)$$

where T is the age in Ga and λ=0.00654 Ga^{-1}.

The $\in_{Nd}$ of a rock at any time in the past depends on the integrated Sm/Nd ratio of the rock and its source material. The Earth formed with chondritic concentrations of both Sm and Nd. As it differentiated, Nd was preferentially extracted into the crust relative to Sm due to the former's greater imcompatibility in mantle melts, thus crustal rocks generally have low Sm/Nd ratios whereas the Sm/Nd ratio of the mantle has increased over time. Because of this, the crust and mantle have evolved different $\in_{Nd}$ values over the history of the Earth as ^{147}Sm decays to ^{143}Nd. Today, the crust has an average $\in_{Nd}$ value of –12, with a wide range depending on the mineralogy and mixing with mantle rocks (DePaolo 1988). The depleted mantle (that portion of the mantle from which crustal material has been extracted) has a present-day average $\in_{Nd}$ value of about +8 (DePaolo et al., 1991). Several different models have been proposed for the Nd isotopic evolution of the depleted mantle (*e.g.*, DePaolo, 1981; Goldstein et al., 1984), and there is some evidence for extreme $\in_{Nd}$ values ranging from +5 to –1 during early (>3.8 Ga) mantle diffentiation (Bennett et al., 1993; Bowring and Housh, 1995), although this has been vigorously disputed (Moorbath et al., 1997). Overall, the average depleted mantle is thought to have evolved

nearly monotonically over most of the history of the Earth, and $\in_{Nd}$ of depleted mantle at any time in the past can be conveniently calculated as follows (DePaolo et al., 1991):

$$\varepsilon_{Nd}(T) = 8.6 - 1.91T \quad (1.3)$$

where T is age of the mantle in Ga.

Ultramafic rocks generally originate from depleted mantle sources, either as residues of partial melting or as cumulates formed from fractional crystallization in a layered mafic intrusion. Because of their unique mineralogy, ultramafic rocks often have very high Sm/Nd ratios, higher even than depleted mantle (*e.g.*, Sharma et al., 1995), and so can evolve to very high $\in_{Nd}$ values.

Weathering processes have been shown to further fractionate Sm and Nd (Banfield and Eggleton, 1989; MacFarlane et al., 1994), and may even "reset" the Sm-Nd isotope systematics (*i.e.*, isotopically homogenize the profile) to the age of soil formation (Stafford et al., 2001). Metasomatism and high metamorphic temperatures may disrupt the Sm-Nd system in a rock (Moorbath et al., 1997), completely resetting the age or just scattering the data.

1.2.6. Rb-Sr system

Strontium is a member of the alkaline earth group IIA. It substitutes readily for calcium in many minerals, especially Ca-carbonate, Ca-sulfate, and plagioclase feldspar. Strontium has four naturally occurring stable isotopes: ^{88}Sr, ^{87}Sr, ^{86}Sr and ^{84}Sr. Three of the four isotopes occur in constant proportions, whereas the other, ^{87}Sr, has variable abundance due to the decay of ^{87}Rb by beta emission and with a half-life of 48.8 billion years. The parent element, rubidium, is an alkali metal. It can substitute for potassium in all K-bearing minerals (Faure, 1986). Rocks with higher Rb/Sr ratios will over time develop higher $^{87}Sr/^{86}Sr$ ratios. The concentration of Rb in ultramafic

rocks is many orders of magnitude less than the concentration in crustal rocks. Over time, ultramafic rocks will develop higher $^{87}Sr/^{86}Sr$ ratios as ^{87}Rb decays, but this ratio will increase at a much slower rate than other normal crustal rocks with higher Rb concentrations. The Rb-Sr system is generally thought to be susceptible to disruption by low-grade metamorphism or weathering (Macfarlane and Holland, 1991), whereas the Sm–Nd system is generally considered more robust (Faure, 1986; DePaolo, 1988).

2. SAMPLE PREPARATION METHODS AND RESULTS

2.1. Sample Preparation and Isotopic Results

2.1.1. Sample Chemistry

A total of eight Kalkkloof sample powders were provided by Dr. H. Ohmoto and Dr. Y. Watanabe. Of these, seven were from the weathering profile and one (KL-2) is considered parent material. About 500 milligrams (mg) of the eight samples were dissolved in a mixture of hydrofluoric (HF) and perchloric ($HClO_4$) acids in closed, heated Teflon vials. The samples were fluxed at ~100°C on a hot plate overnight. After fluxing, the vials were cooled, uncapped and put back on the hot plate to dry at ~120°C for about 8 hours, ~165°C for about 8 hours, and ~195°C until completely dry. Once the samples were cool, 6N hydrochloric acid was added to each sample and checked for clarity to make sure the sample was completely dissolved. If the sample was not clear, the HF + $HClO_4$ mixture was added again and the heating and drying procedure above was repeated. If the sample was clear, it was evaporated to dryness. Each sample was then redissolved in 4N nitric acid and centrifuged for ten minutes at 4000 rpm to remove any possible precipitates. A mixed element tracer solution containing ^{87}Rb, ^{84}Sr, ^{147}Sm and ^{150}Nd was added to a small aliquot of each sample. This was loaded onto a rhenium filament to determine approximate concentrations of Rb, Sr, Sm, and Nd by isotope dilution thermal ionization mass spectrometry. Once these concentrations were known, high-purity ^{87}Rb-^{84}Sr and ^{147}Sm-^{150}Nd mixed tracer solutions were added to each sample, the solutions were evaporated to dryness, and the residue was re-dissolved in 1.5 N HCl.

The samples were eluted through cation exchange columns with AG50W X 16 resin to separate the Rb, Sr, and rare earth elements as a group. The Sr portion was run through a small

(100 μL) quartz column containing Sr-selective resin (SrSpec ®) to further purify the strontium. The REE portion was run through a rare earth element column with LN Spec® resin to separate Sm and Nd from the other REE and each other.

2.1.2. Mass spectrometry

A portion (1/10-1/100) of the Rb cut from the cation column was loaded directly onto a rhenium (Re) filament and $^{85}Rb/^{87}Rb$ was measured by thermal ionization mass spectrometry (TIMS) on the University of Pittsburgh MAT 262 instrument using an ion counter. Because Rb has only two isotopes, mass fractionation cannot be corrected during the run; therefore, the measurement uncertainty is estimated to be ~1% of the measured ratio (larger than the in-run uncertainty by a factor of 5-10).

Approximately 250 ng of separated Sr was loaded on a Re filament with tantalum oxide and run by TIMS. All four isotopes of Sr were measured simultaneously by Faraday collector along with ^{85}Rb to monitor interference of ^{87}Sr from ^{87}Rb. Beam intensities for ^{88}Sr were 2 to 4 x 10^{11} amps (A). Mass fractionation was corrected using an exponential law assuming $^{86}Sr/^{88}Sr = 0.1194$. During most runs, the in-run statistics produced uncertainties better than 15 ppm. Our estimated external reproducibility is 20 ppm. The concentration was determined by isotope dilution simultaneously with the isotopic composition, and the overall uncertainty in the $^{87}Rb/^{86}Sr$ ratio is determined primarily by the Rb measurement uncertainty (~1-2% of the ratio).

Separated samarium (30-100 ng) was loaded onto Re double filaments and all isotopes were measured by simultaneously on Faraday collectors. Mass fractionation was corrected using an exponential law with $^{149}Sm/^{152}Sm = 0.51686$. Beam intensities for ^{152}Sm were in the range of 0.1

to 0.3 x 10^{11} A. Based on in-run statistics, the concentration of Sm was generally determined to much better than ±0.05%.

The spiked Nd cut was loaded on a double Re filament and run in a similar manner as Sm. The isotopes ^{142}Nd, ^{143}Nd, ^{144}Nd, ^{145}Nd, ^{146}Nd, and ^{150}Nd were measured simultaneously on Faraday collectors, with ^{144}Nd intensities in the range of 0.8 to 2 x 10^{11} A. ^{147}Sm was monitored continuously on a Faraday collector to correct for interference from ^{144}Sm and ^{150}Sm. Mass fractionation was corrected using an exponential law with ^{146}Nd/^{144}Nd = 0.724134. In-run uncertainties of the measured ^{143}Nd/^{144}Nd ratio for most samples were on the order of 10-15 ppm; the one exception is sample KL-11, which had an in-run uncertainty of ~30 ppm, due to the small sample size. Neodymium concentrations were determined simultaneously with isotopic composition, and uncertainties were <±0.01% of the measured value. We conservatively estimate the uncertainty in the ^{147}Sm/^{144}Nd ratio to be 0.2% of the measured value, to take into account all possible sources of error in both runs, as well as spike calibration uncertainties.

2.2. Radiogenic isotope results

2.2.1. Sm-Nd System

The Sm concentrations range from 0.020 to 1.6 ppm, and Nd concentrations from 0.067 to 9.7 ppm (Table 2-1). Element mobilities in the weathering horizons can be evaluated by relating that element to the parent rock and to an immobile element using the equation:

$$\%Change = \left[\frac{(X/I)_{sample}}{(X/I)_{parent}} - 1 \right] * 100 \qquad (2.1)$$

where X is the element being analyzed and I is the immobile element (Nesbitt, 1979). This calculation shows the accumulation or depletion of an element relative to the parent rock by

pedogenic or other processes. Variations in Ti-normalized Sm and Nd concentrations are shown in Figure 2-1. In all of the samples, Sm and Nd are enriched relative to the parent, and Nd is enriched to a greater extent than Sm. The largest enrichments are at the bottom of the paleosol, which is consistent with accumulation of REE at the base of the profile through weathering processes.

Table 2-1: Kalkkloof Sm-Nd isotope data.

Sample	Depth (m)[a]	Sm (ppm)	Nd (ppm)	$^{143}Nd/^{144}Nd$ (m)	$^{147}Sm/^{144}Nd$[b]	epsilon Nd (T)[c,d]
KL-17	0.5	0.465	2.873	0.510553 ± 5	0.0978	6.59 ± 0.13
KL-16	1.0	0.047	0.187	0.510572 ± 6	0.1525	-10.74 ± 0.17
KL-13	4.5	0.172	0.724	0.510585 ± 7	0.1437	-7.64 ± 0.18
KL-11	6.5	0.020	0.067	0.513082 ± 14	0.1776	30.45 ± 0.33
KL-5	11.5	1.227	6.937	0.510890 ± 7	0.1070	10.25 ± 0.17
KL-4	12.0	0.296	1.365	0.511091 ± 7	0.1310	6.42 ± 0.18
KL-3	13.5	1.57	9.66	0.510877 ± 7	0.0984	12.78 ± 0.17
KL-2	14.0	0.04	0.12	0.511680 ± 8	0.1969	-3.36 ± 0.22

a: Depth below top of exposed profile

b: Estimated uncertainty is <0.2% of the measured $^{147}Sm/^{144}Nd$ ratio

c: Age of 2.5 Ga does not necessarily represent the age of the paleosol; it is in the middle of the possible age ranges for pedogenesis

d: λ_{Sm} = 0.00654 and chondrite $^{143}Nd/^{144}Nd(0)$ = 0.511847

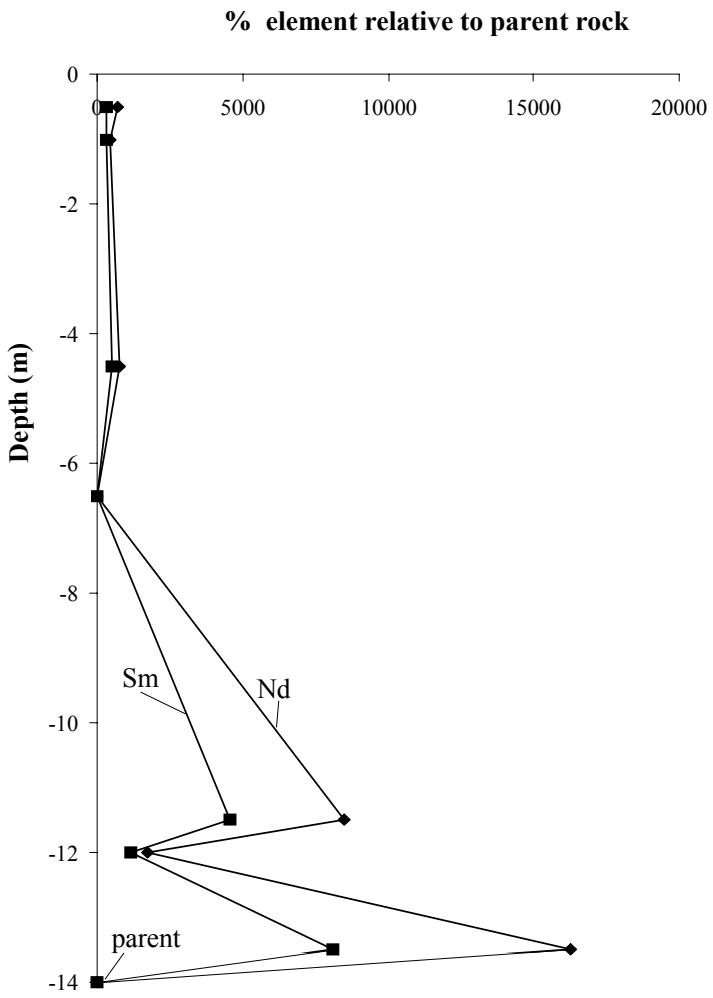

Figure 2-1: Percent increase in Sm and Nd (normalized to Ti) relative to Kalkkloof paleosol parent material. Ti concentrations from Watanabe (personal communication, 2004).

All but one sample (KL-2) have $^{147}Sm/^{144}Nd$ ratios lower than that of chondrites (0.1967). ϵ_{Nd} values show a wide range of about 50 ϵunits, from -25.3 to +24.1. A key issue in applying Nd isotopes to Precambrian paleosols is determining an age to which present-day $^{143}Nd/^{144}Nd$ ratios can be corrected for ^{147}Sm decay.

The Sm-Nd system may record an approximate age of pedogenesis of paleosols as shown by Stafford et al. (2000, 2001). In Figure 2-2, the Sm-Nd data are plotted in a standard isochron-type diagram. A linear regression through the data yields an "age" of 1.7±1.5 Ga, but the high degree of scatter in the plot clearly shows that this age is not geologically meaningful. For comparison, isochrons corresponding to ages of 2.5 Ga (possible age of pedogenesis) and 3.4 Ga (approximate age of ultramafic parent material) are shown. If the Sm-Nd system was homogenized during either of these events, then it has clearly been subsequently disturbed to a large extent.

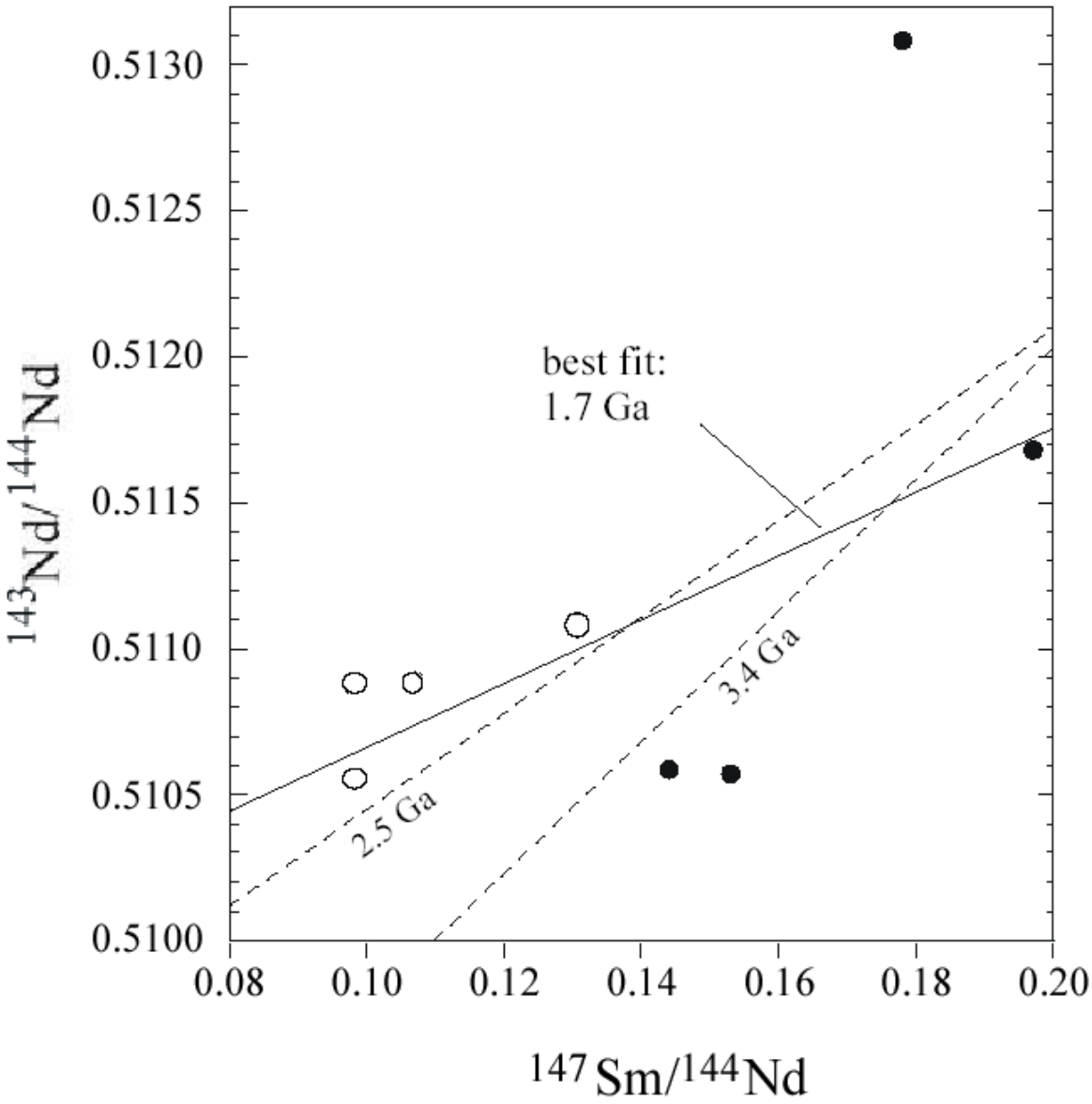

Figure 2-2: Sm/Nd isochron plot for Kalkkloof paleosol samples. The solid line is the "best fit" curve, and the dashed lines represent isochrons calculated for ages of 2.5 and 3.4 Ga, with initial $^{143}Nd/^{144}Nd$ ratios equal to depleted mantle at the calculated age. The best fit curve is not thought to have any age significance. Open circles represent the samples with the Ce anomalies.

The results may indicate that the whole-rock $^{143}Nd/^{144}Nd$ was never homogenized, either at the time of formation of the layered ultramafic parent body or during weathering and soil formation. To examine this possibility, variations in $\epsilon_{Nd}(T)$ are shown as a function of depth in the profile for ages of 2.5 and 3.4 Ga (Fig. 2-3). At 3.4 Ga, mantle-derived ultramafic material (which may itself be residual mantle) would be expected to have an $\epsilon_{Nd}(T)$ value of about +2 (Eqn. 1.2). None of the 3.4 Ga-corrected values (Fig. 2-3) fall within the range of 0 to +5, suggesting that no samples have remained undisturbed since the formation of the ultramafic parent body, including the paleosol parent rock, KL-2 (14 m depth). By 2.5 Ga, individual units within the parent layered body could have evolved a wider range of $\epsilon_{Nd}(T)$ values, due to variations in the Sm/Nd ratios of the parent rock. As discussed in Chapter 1, ultramafic materials generally have Sm/Nd ratios greater than those of chondrites, and so would be expected to evolve toward higher ϵ_{Nd} values. Given the likely maximum and minimum Sm/Nd ratios for ultramafic rocks, $\epsilon_{Nd}(2.5\ Ga)$ values in the range of 0 to +15 might be expected. Four of the samples corrected to 2.5 Ga lie within this range (Fig. 2-3), and the rest fall outside of likely ϵ_{Nd} values for this time period, although the one high ϵ_{Nd} value (KL-11, at 6.5 m depth) could be consistent with a very depleted, high Sm/Nd ultramafic rock. The samples that fall within the "acceptable" ϵ_{Nd} range at 2.5 Ga could plausibly be preserving pedogenic Nd isotope ratios.

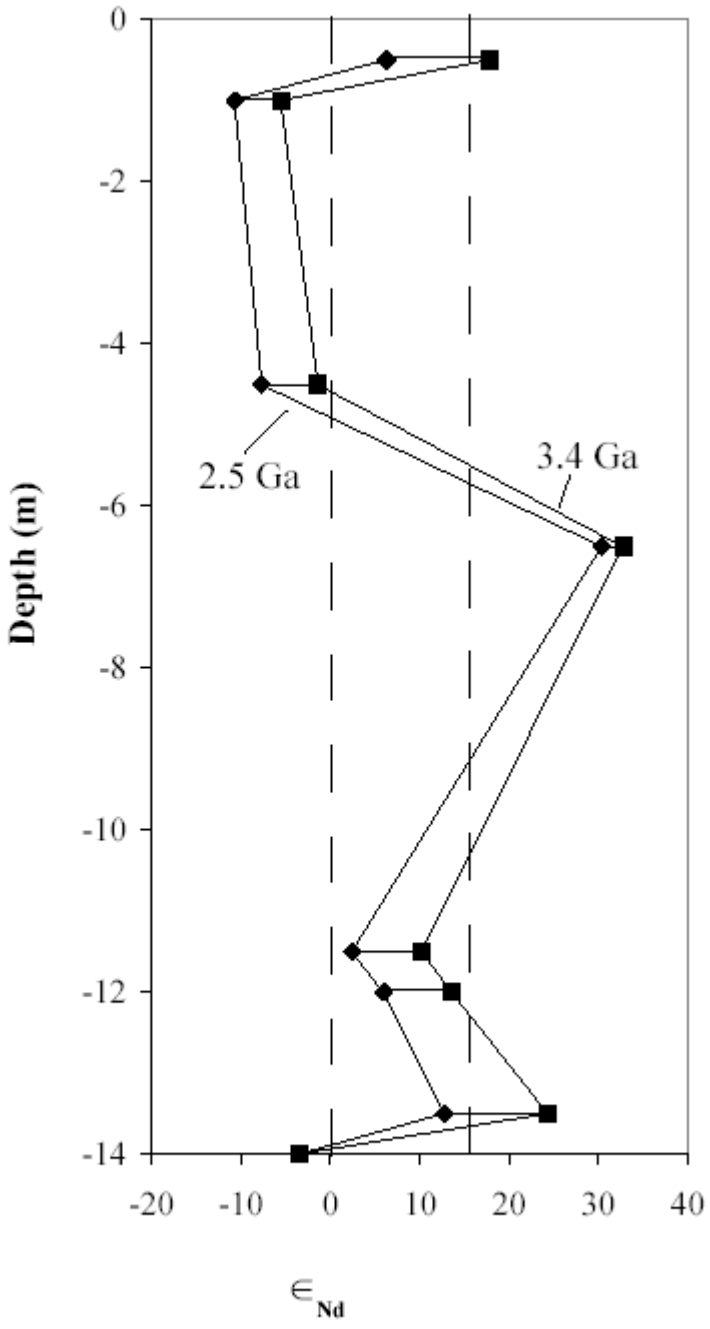

Figure 2-3: ϵ_{Nd} (T) vairations with depth. The curve on the left ϵ_{Nd} is calculated for T = 2.5 Ga and the curve on the right for T = 3.4 Ga. The dashed lines represent the range of expected values for this 2.5 Ga ago period. Open symbols represent the samples with Ce anomalies.

2.2.2. Rb-Sr system

The rubidium concentrations range from 0.086 to 4.3 ppm. The strontium concentrations range from 0.24 to 5.1 ppm (Table 2-2). Sample KL-11 has the lowest concentration of these elements and sample KL-17 has the highest concentration. Without these end members, the ranges are significantly smaller: 0.12 to 0.53 ppm for Rb and 0.50 to 1.3 ppm for Sr. The $^{87}Rb/^{86}Sr$ ratios are high compared to most ultramafic rocks (*e.g.*, Stewart and DePaolo, 1990, 1996), ranging from 0.71 to 2.5, with KL-2 having the lowest value and Kl-17 having the highest value. Gains and losses of Rb and Sr compared to the parent rock using equation 2.1 are shown in Figure 2-4. Concentrations of Rb and Sr behave similarly; both have been added to the section, with Rb showing a greater amount of enrichment. In particular, sample KL-17 at the top of the examined section shows an enrichment in Rb of >1000%.

Table 2-2: : Kalkkloof Rb-Sr isotope data

Sample	Depth (m)[a]	Rb (ppm)	Sr (ppm)	$^{87}Rb/^{86}Sr$[b]	$^{87}Sr/^{86}Sr$ (0 Ga)[c]	$^{87}Sr/^{86}Sr$ (2.5 Ga)[d]
KL-17	0.5	4.30	5.08	2.48	0.827676 ± 10	0.7381
KL-16	1	0.232	0.576	1.17	0.748266 ± 40	0.7059
KL-13	4.5	0.535	1.10	1.42	0.760949 ± 10	0.7097
KL-11	6.5	0.086	0.240	1.04	0.735498 ± 12	0.6980
KL-5	11.5	0.334	0.820	1.18	0.729213 ± 14	0.6862
KL-4	12	0.153	0.388	1.15	0.731154 ± 14	0.6897
KL-3	13.5	0.337	1.32	0.738	0.728632 ± 11	0.7019
KL-2	14	0.122	0.496	0.714	0.728028 ± 24	0.7022

. a: Depth below top of exposed profile

b:The estimated uncertainty of $^{87}Rb/^{86}Sr$ is 1% of the measured value

c: The uncertainty shown is 2σ in-run standard deviation. Estimated external reproducibility is 20 ppm

d: The age of 2.5 does not represent the age of the paleosol; it is in the middle of the possible age ranges

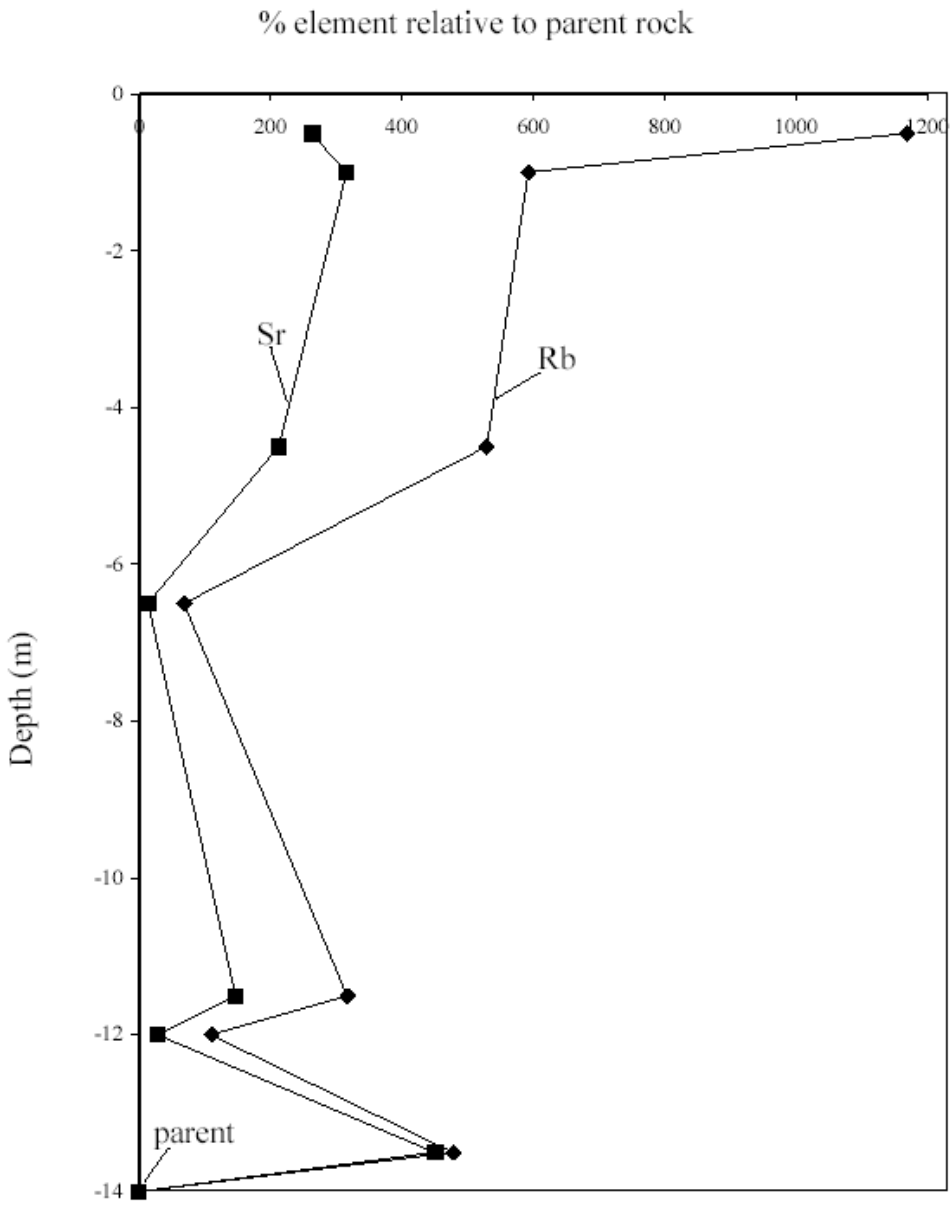

Figure 2-4: Percent increase in Rb and Sr (normalized to Ti) relative to Kalkkloof paleosol parent material. Ti concentrations from Watanabe (personal communication, 2004).

Measured $^{87}Sr/^{86}Sr$ ratios vary from 0.72803 to 0.82768, with KL-17 from the top of the paleosol having a significantly higher value than the rest of the samples. To reach the high $^{87}Sr/^{86}Sr$ ratios measured today, these samples are likely to have evolved at high Rb/Sr ratios for >2 Ga.

As with the Sm-Nd system, we plot the Rb-Sr data in an isochron diagram to determine whether or not the Rb-Sr system yields meaningful age information (Fig. 2-5). Whereas the linear correlation is stronger than that shown by the Sm-Nd data, yielding an age of 4.0±1.5 Ga, the scatter of the data clearly do not allow age interpretation. Moreover, the calculated initial $^{87}Sr/^{86}Sr$ of 0.679±0.022 is lower than the initial bulk Earth value (0.698), which clearly indicates one or more disturbances to the Rb-Sr system subsequent to the early Archean.

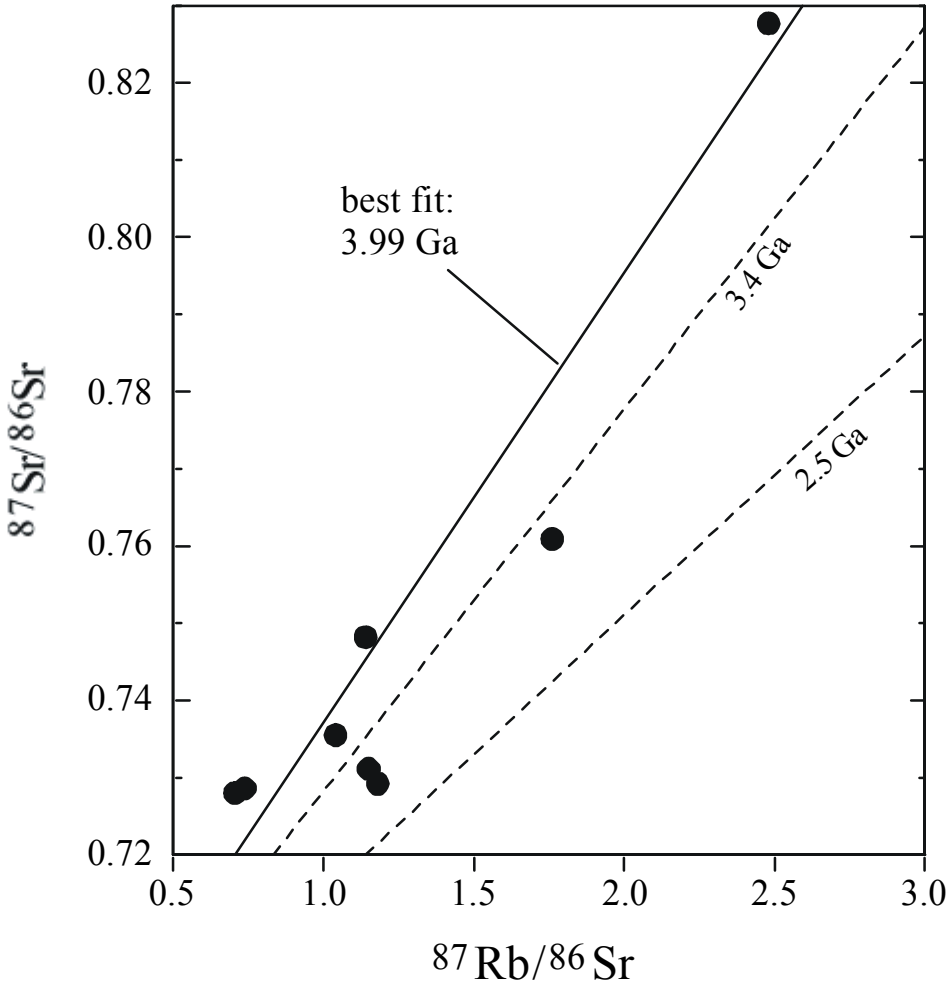

Figure 2-5: Rb-Sr isochron diagram for Kalkkloof samples. Shown for reference are isochron curves for ages of 2.5 and 3.4 Ga, with the same initial $^{87}Sr/^{86}Sr$ as the best fit curve of 3.99 Ga. The best fit curve, with an initial $^{87}Sr/^{86}Sr$ of 0.679, is not thought to have age significance.

In Figure 2-6, initial $^{87}Sr/^{86}Sr$ is plotted against depth in the paleosol for the ages of 2.5 Ga and 3.4 Ga. At 3.4 Ga, an expected range in $^{87}Sr/^{86}Sr$ for mantle-derived materials would be 0.700 to 0.701. Only one sample has a ratio corrected to 3.4 Ga that is close to these values (KL-17, with $^{87}Sr/^{86}Sr = 0.705$). Many of the samples have ratios below the initial bulk Earth ratio. At 2.5 Ga, there is a wider range of permissible $^{87}Sr/^{86}Sr$ values for the evolved ultramafic rocks, from about 0.701 to 0.705. Three samples, KL-2, KL-3, and KL-16, fall near these values, while four samples lie well below allowable $^{87}Sr/^{86}Sr$ ratios, and one (KL-17) corrects to an unreasonably high value for 2.5. Ga of 0.738. Taken together, these data show that the scatter in the isochron (Fig. 2-5) cannot simply reflect initial isotopic heterogeneity in either the ultramafic parent body or in the subsequent weathering profile. Rather, there must have been one or more later disturbances to the Rb-Sr system.

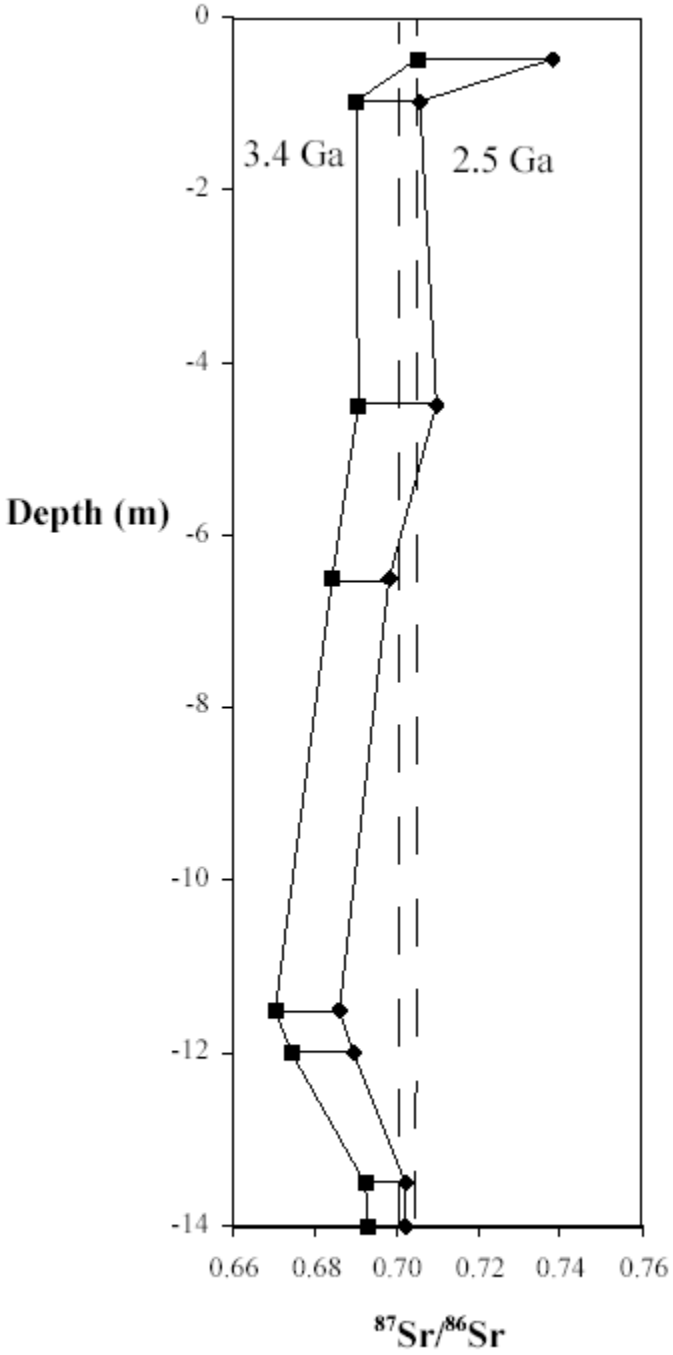

Figure 2-6: Plot of $^{87}Sr/^{86}Sr(T)$ variations with depth in the Kalkkloof profile. The curve on the right is calculated for T = 2.5 Ga, and the one on the left for T = 3.4 Ga. The dashed lines represent the range of expected values.

3. DISCUSSION AND CONCLUSIONS

3.1. Discussion

3.1.1. Sm-Nd systematics and REE mobility during pedogenesis

A key issue in studying Precambrian paleosols is the degree to which geochemical signatures of weathering processes are preserved to the present day. In the case of the Kalkkloof paleosol, an important observation is the occurrence of cerium anomalies in the rare earth element patterns (Watanabe et al., 2003; Watanabe, personal communication, 2004), which signal the presence of an oxygen-rich atmosphere at the time of formation. Because Sm and Nd are rare earth elements, the degree of preservation of Sm-Nd systematics can be considered a guide for interpreting the preservation of REE patterns, including Ce anomalies. The Sm-Nd systematics of samples measured in this study show clear evidence of post-2.5 Ga disturbance. However, when $\in_{Nd}$ is corrected to 2.5 Ga, a few of the samples yield reasonable values consistent with the evolution of ultramafic rock units from 3.4 Ga to the time of pedogenesis (Fig. 2-3). These samples (KL-3, 4, 5 and 17) all have Nd concentrations greater than 1 ppm (Fig. 3-1), and show the most significant Ce anomalies (Watanabe et al., 2003; Watanabe, personal communication, 2004). These results support the interpretation that these samples preserve pedogenic REE concentrations and Sm-Nd ratios. Isotopic ratios and REE concentration patterns can be easily modified by elemental exchange during metamorphism when the rocks have low concentrations (< 1ppm) of these elements. The REE in rocks with higher concentrations could be held in relatively resistant phosphate minerals, which could make the REE and Sm-Nd system more impervious to post-pedogenic resetting and remobilization processes such as metamorphism.

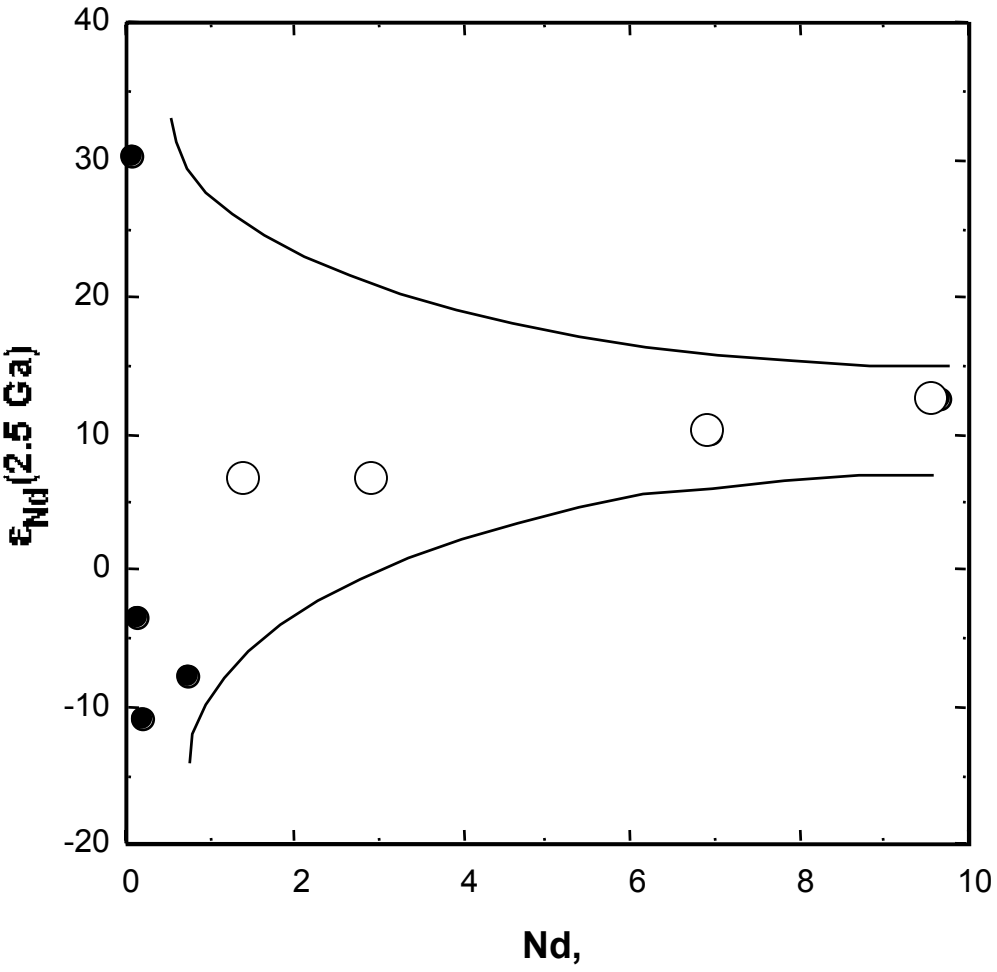

Figure 3-1: $\in_{Nd}$ values of Kalkkloof samples corrected to 2.5 Ga plotted against Nd concentration. Note the range of ε_{Nd} values converges with higher Nd concentrations. Open circles are samples with Ce anomalies.

3.1.2. Modeled Sm-Nd evolution of Kalkkloof paleosol samples

The results show that whereas some of the Kalkkloof whole rock samples might preserve pedogenic REE chemistry, others clearly do not, and none of the samples has survived unaltered from the time of formation of the ultramafic parent body. Therefore, the Kalkkloof paleosol itself has undergone at least three different "events" that affected its geochemistry, possibly including (1) formation of the parent body, (2) pedogenesis, and (3) subsequent metamorphism. The Nd isotopic evolution of each of the samples over the past ~4 Ga is shown in Figure 3-2a. As shown,

there is no convergence about mantle or depleted mantle values at any time over the history of the Kalkkloof samples, if their evolution is plotted using present-day ϵ_{Nd} and $^{147}Sm/^{144}Nd$ values.

A conceptual model for the Nd isotope evolution of the Kalkkloof paleosol is presented in Figure 3-2b. This is not a unique model, nor does it provide specific information about the timing of pedogenesis, but it is consistent with the data and with what is known about the Kalkkloof paleosol. According to this model, the layered ultramafic parent body forms from a depleted mantle source at 3.4 Ga with an initial ϵ_{Nd} value of +2 (eqn. 1.2). Individual layers within the ultramafic complex might have different initial Sm/Nd ratios and would be expected to evolve along trajectories defined by their individual Sm/Nd ratios, which should in general be greater than or equal to the Sm/Nd of depleted mantle. Thus, by the time pedogenesis takes place (assumed here to be at ~2.5 Ga ago), there would be a spread in ϵ_{Nd} values, with most greater than that of depleted mantle. Weathering reactions at 2.5 Ga resulted in some redistribution of Nd (and mixing of ϵ_{Nd} values) and loss of HREE, including Sm, from most samples. The result is that the Sm/Nd ratio is reduced to a level below that of chondrites. Thus, subsequent to weathering, samples evolve with lower Sm/Nd ratios. At a later time, modeled here to be coincident with the ca. 2 Ga metamorphism associated with intrusion of the Bushveld Complex, evolutionary trajectories of some samples are further modified as Sm/Nd ratios are shifted to their present values by addition of Sm or depletion of Nd. As discussed in Section 3.1.1., the samples with the highest REE concentrations may have only been minimally affected by the last metamorphic event.

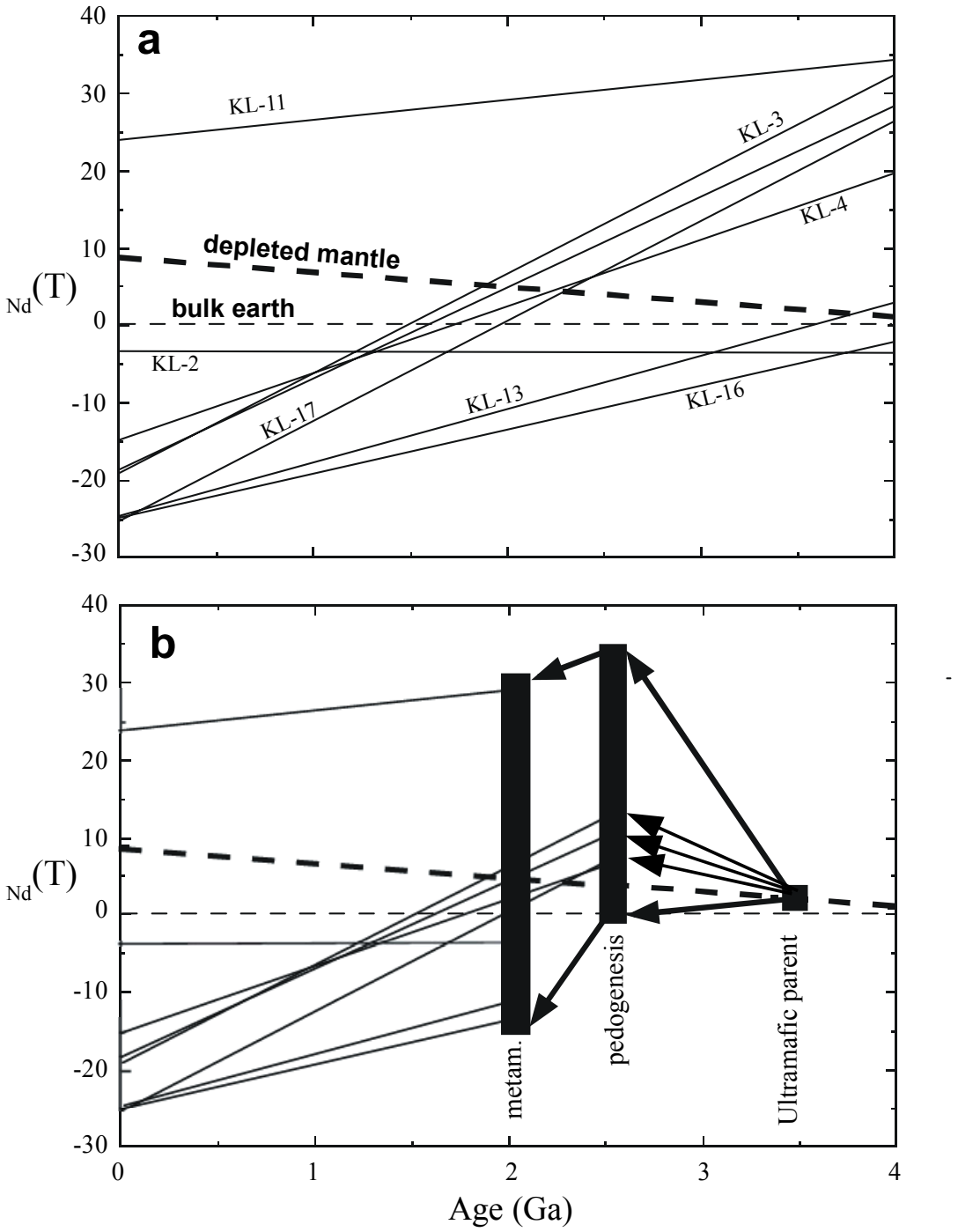

Figure 3-2. Model for ϵ_{Nd} evolution.

a. Projected ϵ_{Nd} values based on present-day $^{143}Nd/^{144}Nd$ and $^{147}Sm/^{144}Nd$ for all Kalkkloof samples. The horizontal dashed line represents bulk earth evolution, and the heavy dashed line is a model curve for depleted mantle evolution (DePaolo et al., 1991).

b. The same plot is shown with trajectory-changing geological events added, including derivation of parent material from the mantle (with variable but high Sm/Nd), pedogenesis (which tends to lower Sm/Nd) and later metamorphism.

3.1.3. Rb-Sr systematics and Sr isotopic evolution

As previously shown, (Section 2.2.2) the Kalkkloof whole rock samples do not define an isochron. That is, there is no single age of Sr isotopic homogenization followed by undisturbed decay of ^{87}Rb to the present day. Trajectories for the evolution of $^{87}Sr/^{86}Sr$ over the past 4 Ga for each of the Kalkkloof samples are shown in Figure 3-3a. The bulk earth $^{87}Sr/^{86}Sr$ value provides a reasonable lower limit for any of the Kalkkloof samples, and the initial Earth $^{87}Sr/^{86}Sr$ at 4.5 Ga (0.698) is an inviolable minimum for any terrestrial sample younger than the age of the Earth. The points where any of the Kalkkloof samples cross these minima represents the maximum age of disturbance or resetting of the Rb-Sr system for that sample. Using these criteria, samples KL-4 and KL-5 must have had their $^{87}Sr/^{86}Sr$ or Rb/Sr ratio disturbed in some sort of event after 1.6-1.7 Ga ago. This could include modern weathering or alteration of the samples, or any event between the present day and ~1.7 Ga. Other samples cross the bulk and initial Earth minima at different times, back to >3.5 Ga ago. The Kalkkloof Rb-Sr systematics were evidently disturbed by multiple events, the latest of which must have taken place no earlier than ~1.7 Ga. It is not surprising that the Rb-Sr system shows disturbances, as (1) both Rb and Sr are considered highly mobile during weathering and metamorphism, and (2) these samples contain rather low concentrations of Sr, making them susceptible to contamination. Unlike some other paleosols (*e.g.*, Macfarlane and Holland, 1991 and Stafford et al., 2001), the Kalkkloof Rb-Sr systematics show no evidence of being completely homogenized and reset by post-pedogenic metamorphism.

A simplified model for $^{87}Sr/^{86}Sr$ evolution is shown in Figure 3-3b. Here, most samples are assumed to have started with a bulk-Earth $^{87}Sr/^{86}Sr$ ratio at 3.4 Ga (derivation of the ultramafic body from the Earth's mantle), and followed low Rb/Sr trajectories typical of ultramafic rocks for the next ~1 Ga. In this model, the isotope systematics are shown to be disturbed during

pedogenesis (around 2.5 Ga ago) and by a later metamorphic event beginning around 2 Ga ago. This event may have been somewhat protracted (to 1.7 Ga) with respect to the easily-disturbed Rb-Sr system. Sample KL-17, which is very near the top of the profile and the overlying shale unit, could have been contaminated by Sr from the shale, which would be expected to have a very high $^{87}Sr/^{86}Sr$.

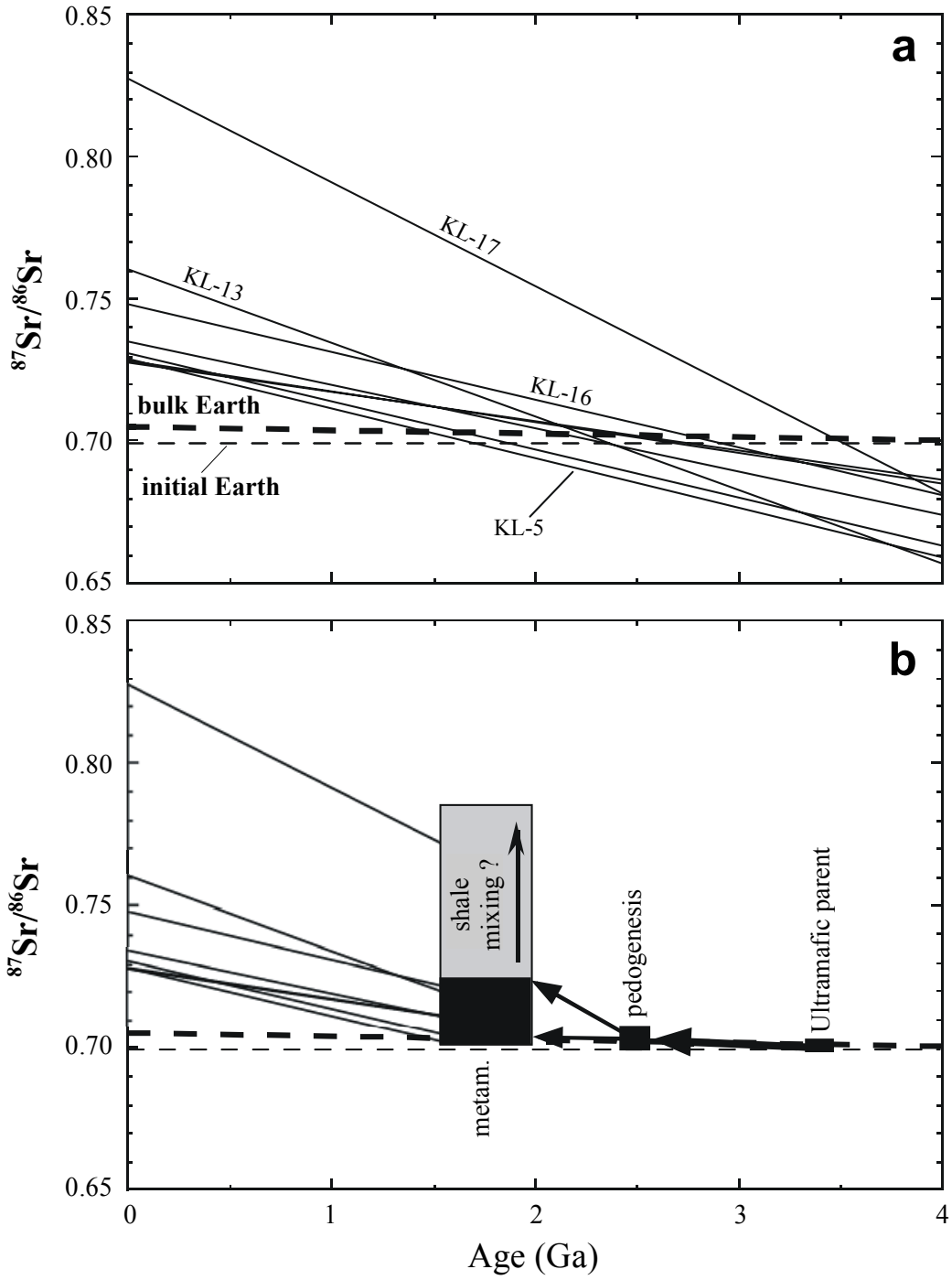

Figure 3-3. Model for Sr evolution.

a. Sr isotope evolution of Kalkkloof samples. The light horizontal dashed line represents the initial Earth $^{87}Sr/^{86}Sr$, and the heavy dashed line is the approximate bulk Earth evolution. Depleted mantle would fall somewhere in between.

b. b. Model for geological events affecting Kalkkloof $^{87}Sr/^{86}Sr$ values, including derivation from the mantle at ~3.4 Ga, pedogenesis at ~2.5 Ga (which would tend to increase Rb/Sr), and metamorphism starting around 2 Ga, which may have been accompanied by Sr exchange with the overlying high $^{87}Sr/^{86}Sr$ shale.

3.2. Conclusions

The Kalkkloof paleosol is a rare example of a Precambrian ultramafic weathering profile. It is of particular importance because weathering took place between ~2.6 and 2.3 Ga ago, possibly during the purported rise of atmospheric oxygen to near present-day levels, and cerium anomalies suggesting high atmospheric O_2 levels are reported in several of the Kalkkloof samples (Watanabe et al., 2003). I applied the Rb-Sr and Sm-Nd isotope systems to better constrain the age of pedogenesis and to evaluate possible post-pedogenic disturbances to paleosol geochemistry. The Sm-Nd and Rb-Sr results lead to the following conclusions:

- Whole-rock Sm-Nd samples do not define the age of any given event affecting the paleosol, whether it was the initial derivation of the parent material from the mantle, development of the weathering profile, or subsequent metamorphism.
- If any samples preserve $^{143}Nd/^{144}Nd$ ratios consistent with the time of profile formation, it is those with the highest REE concentrations, which also are the samples showing the major Ce anomalies. This could suggest that the Ce anomalies formed before 2.3 Ga ago and are not artifacts of post-pedogenic alteration such as metamorphism or modern weathering.
- The Sm-Nd systematics are consistent with at least three-stages in the geochemical evolutionof the Kalkkloof samples, including (1) derivation of parent material from the mantle; (2) formation of a weathering profile; and (3) post-pedogenic metamorphism.
- The Rb-Sr systematics are also consistent with a multiple stage history for the paleosol, and they suggest that the latest disturbance to the system occurred no earlier than ~1.7 Ga

ago - possibly the waning stages of the 2 Ga metamorphism reported for the Kalkkloof region.

BIBLIOGRAPHY

Aubert, D., P. Stille, and A. Probst (2001) REE fractionation during granite weathering and removal by waters and suspended loads: Sr and Nd isotopic evidence. *Geochimica et Cosmochimica Acta* **65,** 387-406.

Banfield, J. and R. Eggleton (1989) Apatite replacement and rare earth mobilization, fractionation, and fixation during weathering. *Clays and Clay Minerals* **37,** 113-127.

Bekker, A., H.D. Holland, P.-L. Wang, D. Rumble III, H.J. Stein, J.L. Hannah, L.L. Coetze, and N.J. Buekes (2004) Dating the rise of atmospheric oxygen. *Nature* **427,** 117-120.

Bennett, V.C., A. P. Nutman, and M. T. McCulloch (1993) Nd evidence for transient, highly depleted mantle reservoirs in the early history of the Earth. *Earth and Planetary Science Letters* **119,** 299-317.

Bowring, S.A. and T. Housh (1995) The Earth's early evolution. *Science* **269**, 1535-1540.

Braun, J.-J., M. Pagel, J.-P. Muller, P. Bilong, A. Michard, and B. Guillet (1990) Cerium anomalies in lateritic profiles. *Geochimica et Cosmochimica Acta* **54,** 781-795.

Braun, J.-J., J. Viers, B. Dupre, M. Polve, J. Ndam, and J.-P. Muller (1998) Solid/liquid REE fractionation in the lateritic system of Goyoum, East Cameroon: The implication for the present dynamics of the soil covers of the humid tropical regions. *Geochimica et Cosmochimica Acta* **62,** 273-299.

Braun, J.-J., M. Pagel, A. Herbillon, and C. Rosin (1993) Mobilization and redistribution of REEs and thorium in a syenitic lateritic profile: A mass balance study. *Geochimica et Cosmochimica Acta* **57***,* 4419- 4434.

Buick, I.S., R. Uken, R.L. Gibson, and T. Wallmach (1998) High-δ13C Paleoproterozoic carbonates from the Transvaal Supergroup, South Africa. *Geology* **26,** 875-878.

Button, A. and N. Tyler (1981) The character and economic significance of Precambrian paleoweathering and erosion surfaces in southern Africa. *Economic Geology 75th anniversary volume,* 686-709.

Byerly, Gary R. (1999) Komatiites of the Mendon Formation: Late-stage ultramafic volcanism in the Barberton Greenstone Belt. In *Geologic Evolution of the Barberton Greenstone Belt, South Africa*. (ed Donald R. Lowe and Gary Byerly) The Geological Society of America, 189-212.

Clark, A.M. (1984). Mineralogy of the rare earth elements. In *Rare Earth Element Geochemistry.* (ed P. Henderson) Elsevier, 33-62.

Condie, K.C., J. Dengate, and R.L. Cullers (1995) Behavior of rare earth elements in a paleoweathering profile on granodiorite in the Front Range, Colorado, USA. *Geochimica et Cosmochimica Acta* **59,** 279-294.

Condie, K.C. and D.J. Wronkiewicz (1990) The Cr/Th ratio in Precambrian pelites from the Kaapvaal Craton as an index of craton evolution. *Earth and Planetary Science Letters* **97***,* 256-267.

Cullers, R.L. and J.L. Graf (1984) Rare earth elements in igneous rocks of the continental crust: Predominantly basic and ultrabasic rocks. In *Rare Earth Element Geochemistry* (ed. P. Henderson) Elsevier, 237-274.

Depaolo, D.J. (1981) Neodymium isotopes in the Colorado Front Range and crust-mantle evolution in the Proterozoic. *Nature* **291**, 193-196.

DePaolo, Donald J. (1988) *Neodymium Isotope Geochemistry,* Springer-Verlag.

DePaolo, D.J., A.M. Linn, and G. Schubert (1991) The continental crustal age distribution: Methods of determining separation ages from Sm-Nd isotopic data and application to the southwestern United States. *Journal of Geophysical Reasearch* **96**, 2071-2088.

Farquhar, J., S. Airieau, M.H. Thiemens (2001) Observation of wavelength-sensitive mass-independent sulfur isotope effects during SO2 photolysis: Implications for the early atmosphere. *Journal of Geophysical Research* **106,** 32829-32839.

Faure, Gunter (1986) *Principles of Isotope Geology, 2nd ed.* John Wiley and Sons.

Frey, F.A. (1984) Rare earth elements in upper mantle rocks. In *Rare Earth Element Geochemistry (*ed P. Henderson) Elsevier, 153-204.

German, C. and H. Elderfield (1990) Application of the Ce anomaly as a paleoredox indicator: The ground rules. *Paleooceanography* **5,** 823-833.

Goldsten, S.L., R.K. O'Nions, and P.J. Hamilton (1984) A Sm-Nd isotopic study of atmospheric dusts and particulates from major river systems. *Earth and Planetary Science Letters* **70**, 221-236.

Gutzmer, J. and N.J. Buekes (1998) Earliest laterites and possible evidence for terrestrial vegetation in the Early Proterozoic. *Geology* **26,** 263-266.

Hamilton, P. J., N.M. Evenson, R.K. O'Nions, H.S. Smith, and A.J. Erlank (1979) Sm-Nd dating of Onverwacht Group volcanics, Southern Africa. *Nature* **279**, 298-300.

Haughton, S. H. (1969) *Geological History of Southern Africa*. Geological Society of South Africa.

Henderson, P. (1984) General geochemical properties and abundances of the rare earth elements. In *Rare Earth Element Geochemistry* (ed P. Henderson) Elsevier, 1-32.

Holland, H.D. (1984) *The Chemical Evolution of the Atmospheres and Ocean.* Princeton University Press.

Humphris, S. E. (1984) The mobility of the rare earth elements in the crust. In *RareEarth Element Geochemistry* (ed P. Henderson), Elsevier, 317-342.

Jahn, B.-m., J. Berstrand-Sarfati, N. Morin, and J. Mace (1990) Direct dating of stromatilitic carbonates from the Schmidtsdrif Formation (Transvaal Dolomite), South Africa, with implication on the age of the Ventersdorp Supergroup. *Geology* **18,** 1211-1214.

Jahn, B.-M., G. Gnuau, and A.Y. Glickson (1982) Komatiites of the Onverwacht Group, S. Africa: REE geochemistry, Sm/Nd age, and mantle evolution. *Contributions to Mineralogy and Petrology* **80,** 25-40.

Jonasson, R.G., G.M. Bancroft, and H.W. Nesbitt (1985) Solubilities of some hydrous REE phosphates with implications for diagenesis and sea water concentrations. *Geochimica et Cosmochimica Acta* **49,** 2133-2139.

Karhu, J.A. and H.D. Holland (1996) Carbon isotopes and the rise of atmospheric oxygen. *Geology* **24,** 867-870.

Klein, C., and N.J. Beukes (1990) Geochemistry and sedimentology of a facies transition from limestone to iron-formation deposition in the Early Proterozoic, Transvaal Supergroup, South Africa. *Economic Geology* **84,** 1733 - 1774.

Lambert, I.B. T.H. Donnelly (1991) Atmospheric oxygen levels in the Precambrian: a review of isotopic and geological evidence. *Palaeogeography, Palaeoclimatology, Palaeoecology* **97,** 83-91.

Lowe, D.R. and G.R. Byerly (1999) Stratigraphy of the west-central part of the Barberton Greenstone Belt, South Africa. In *Geologic Evolution of the Barberton Greenstone Belt, South Africa* (ed. Lowe, Donald R. and Gary R. Byerly), p. 1-36 The Geological Society of America.

Macfarlane, A. W., A. Danielson, H.D. Holland, and Stein B. Jacobsen (1994) REE chemistry and Sm-Nd systematics of late Archean weathering profiles in the Fortescue Group, Western Australia. *Geochimica et Cosmochimica Acta* **58,** 1777-1794.

Martini, J. E. J. (1994) A late Archean-Paleoproterozoic (2.6 Ga) palaeosol on ultramafics in the Eastern Transvaal, South Africa. *Precambrian Research* **67,** 159-180.

Melcher, F., T. Meisel, J. Puhl, and F. Koller (2002) Petrogenesis and geotectonic setting of ultramafic rocks in the Eastern Alps: constraints from geochemistry. *Lithos* **65,** 69-112.

Menell, R. P., T.H. Brewer, J.R. Delve, and C.R. Anhaeusser (1986) The geology of the Kalkkloof chrysotile asbestos deposit and surrounding area, Barberton Mountain Land. In *Mineral deposits of Southern Africa* (ed. C.R. Anhaeusser and S.Maske) Geological Society of South Africa, 427-435.

Moorbath, S., M.J. Whitehouse, and B.S. Kamber (1997) Extreme mantle heterogeneity in the early Archean - fact or fiction? Case histories from northern Canada and West Greenland. *Chemical Geology* **135,** 213-231.

Murakami, T., S. Utsunomiya, Y. Imazu, and N. Prasad (2001) Direct evidence of late Archean to early Proterozoic anoxic atmosphere from a product of 2.5 Ga old weathering. *Earth and Planetary Science Letters* **15,** 523-528.

Nesbitt, H. W. (1979) Mobility and fractionation of rare earth elements during weathering of a granodiorite. *Nature* **279,** 206-210.

Ohmoto, H. (1996) Evidence in pre-2.2 Ga paleosol for the early evolution of atmospheric oxygen and terrestrial biota. *Geology* **24,** 1135-1138.

Ottonello, G., G.B. Piccardo, and W.G. Ernst (1979) Petrogenesis of some Ligurian peridotites -- II. Rare earth element chemistry. *Geochimica et Cosmochimica Acta* **43,** 1273-1284.

Pan, Y. and M.R. Stauffer (2000) Cerium anomaly and Th/U fractionation in the 1.85 Ga Flin Flon Paleosol: Clues from REE- and U-rich accessory minerals and implications for paleoatmospheric reconstruction. *American Mineralogist* **85,** 898-911.

Panahi, A., G.M. Young, and R.H. Rainbird (2000) Behavior of major and trace elements (including REE) during Paleoproterozoic pedogensis and diagenetic alteration of an Archean granite near Ville Marie, Quebec, Canada. *Geochimica et Cosmochimica Acta* **64**, 2199-2220.

Reimer, T. O. (1988) Carbonaceous high-alumina shale in the Transvaal Supergroup: Evidence of early Proterozoic karstic weathering in a marine environment. In*Early Organic Evolution*. S. G. M. Schidlowski, M.M. Kimberley, D.M. McKirdy, P.A. Trudinger) Springer-Verlag, 106-114.

Rye, R. and H.D. Holland (1998) Paleosols and the evolution of atmospheric oxygen: a critical review. *American Journal of Science* **298,** 621-672.

Sharma, N., G.J. Wasserburg, D.A. Papanastassiou, J.E. Quick, E.V. Sharkov, and E.E. Laz'ko (1995) High 143Nd/144Nd in extremly depleted mantle rocks. *Earth and Planetary Science Letters* **135,** 101-114.

Stafford, S.L., R.C. Capo, B.W. Stewart, and H. Ohmoto (2000) Neodymium isotope investigation of an Archean weathering profile: Steep Rock paleosol, Ontario, Canada. *Geologicical Society of America Abstracts with Program* **32,** A-485.

Stafford, S.L., R.C. Capo, B.W. Stewart, J. Marmo, and H. Ohmoto(2001) Meodymium isotope investigation of a Precambrian weathering profile: Hokkalampi paleosol, north Karelia, eastern Finland. *Proceedings of the 2nd General Meeting of the NASA Astrobiology Institute*, 303-304.

Stewart, B.W. and D.J. DePaolo (1990) Isotopic studies of processes in mafic magma chambers: II. The Skaergaard intrusion, East Greenland. *Contributions to Mineralogy and Petrology* **104,** 124-141.

Stewart, B.W. and D.J. DePaolo (1996) Isotopic studies of processes in mafic magma chambers: III. The Muskox intrusion, Northwest Territories, Canada. In *Earth Processes: Reading the Isotopic Code* (eds A.R. Basu and S.R. Hart) *AGU Monograph* **95,** 277-295.

Suen, C. J. and F.A. Frey (1987) Origins of the mafic and ultramafic rocks in the Ronda Peridotite. *Earth and Planetary Science Letters* **85.** 183-202.

Toulkeridis, T., N. Clauer, A. Kroner, T. Reimer, and W. Todt (1999) Characterization, provenance, and tectonic setting of Fig Tree greywackes from the Archaean Barberton Greenstone Belt, South Africa.*Sedimentary Geology* **124,** 113-129.

Towe, K.M. (2002) The problematic rise of Archean oxygen. *Science* **295**, 1419a.

Towe, K. M. (1991) Aerobic carbon cycling and cerium oxidation: significance for Archean oxygen levels and banded iron formation deposition. *Palaeooceanography, Palaeocimatology, Palaeoecology* **97,** 113-123.

Walraven, F., R. A. Armstrong, and F.J. Kruger (1990) A chronostratigraphic framework for the north-central Kaapvaal craton, the Bushveld Complex and the Vredfort structure. *Tectonophysics* **171,** 23-48.

Walter, A. V., D. Nahon, R. Flicoteaux, J.P. Girard, and A. Melfi (1995) Behavior of major and trace elements and fractionation of REE under tropical weathering of a typical apatite-rich carbonatite from Brazil. *Earth and Planetary Science Letters* **136,** 591-602.

Watanabe, Y., Jacques E.J. Martini, and Hiroshi Ohmoto (2000) Geochemical evidence for terrestrial ecosystems 2.6 billion years ago. *Nature* **408,** 574-578.

Watanabe, Y., T. Nagase and H. Ohmoto (2003) Ce anomalies in the 2.6 – 2.4 Ga Kalkkloof paleosol in South Africa: Evidence for the early development of an oxygenated atmosphere. *13th V.M. Goldschmidt Conference Program with Abstracts,* A528.

Wiechert, U. H. (2003) Earth's early atmosphere. *Science* **298,** 2341-2344.

Yan, X.-P., R. Kerrich, and M.J. Hendry (2001) Distribution of rare earth elements in porewaters from a clay-rich aquitard sequence, Saskatchewan, Canada. *Chemical Geology* **176,** 151-172.

Yang, W., H.D. Holland, and R. Rye (2002) Evidence for low or no oxygen in the late Archean atmosphere from the ~2.76 Ga Mt. Roe #2 paleosol, Western Australia: Part 3. *Geochimica et Cosmochimica Acta* **66,** 3707-3718.